JOURNAL OF MATERIALS SCIENCE 27 (1992) 3036–3042

Bulk and surface characterization of powder iron-doped titania photocatalysts

J. A. NAVIO*, M. MACIAS, M. GONZALEZ-CATALAN, A. JUSTO
Instituto de Ciencia de Materiales, Universidad de Sevilla-CSIC, Apdo. 1115, 41080 Sevilla and Departamento de Química Inorgánica, Facultad de Química, 41012 Sevilla, Spain

Some additional contributions to structural and surface features of powder iron-doped titania photocatalysts have been investigated by applying a variety of complementary techniques: temperature programmed desorption–mass spectrometry analysis, non-isothermal thermogravimetric analysis, differential thermoanalysis, infrared spectroscopy, scanning electron microscopy and X-ray diffraction analysis. The effects of iron concentration and pretreatment temperature, over the polymorphic transformation anatase–rutile, were analysed. The results obtained were used in an attempt to correlate structural and surface aspects of catalysts, with their reported activity versus inactivity to photoreduce dinitrogen to ammonia.

1. Introduction

The search for materials to activate inert species (e.g. nitrogen gas) has become an area of enormous interest. The reaction of dinitrogen photoreduction to ammonia has been considered of particular economical interest, because the Fe–Ti oxide system is one of the more promising systems for the photo-assisted dinitrogen reduction to ammonia [1, 2]. On the other hand, the solid state chemistry of Fe–Ti oxide systems is interesting *per se*; an irreversible crystallographic change from anatase to rutile at elevated preparation temperatures, differences of solubility of iron in those phases, and the formation of pseudobrookite, Fe_2TiO_5, have been found [3]. Considerable effort has been devoted to the study of such systems in order to obtain structure–property relationships which enable the control of end-use properties of those composite materials for dinitrogen photoreduction to ammonia, in order to obtain information about the activity/inactivity of iron-doped titanium dioxide catalysts for such a photo-reaction.

The effect of the iron content on the yield of NH_3, over a series of iron-doped TiO_2 specimens, has been previously investigated [4–6]. A tentative correlation between structural data and reactivity results for this iron-doped titania catalyst, has been pointed out [7–9]. The most active sample was found to be for an iron content of 0.2–0.5 wt % calcined at 773 K. By increasing either or both of the iron content or the calcination temperature, a decrease in the photoactivity was found [4–6].

Differences in photocatalytic activity between iron-loaded and unloaded titania catalysts on the photooxidation of toluene has been reported elsewhere [10].

Although previous results on the characterization of these catalysts have been published [3, 9], we report here additional information about structural phases and surface aspects of these photocatalysts, in particular for the most photoactive sample, 0.5 wt % iron calcined at 773 K.

2. Experimental procedure

2.1. Material and methods

The iron-doped TiO_2 specimens, Fe/TiO_2, were prepared by the wet impregnation method; they are labelled hereafter (IM) x/T, where x is the nominal iron concentration (expressed as percentage of the total cationic content of the TiO_2 matrix; T, the temperature (degrees Kelvin) at which the catalysts were fired in air for 24 h, and IM indicates the impregnation method. The powder TiO_2 sample used in this study was Degussa P-25. Details of the powder preparation and also the characterization by some methods (surface area measurement, diffuse reflectance spectroscopy and ESR spectroscopy), can be found elsewhere [3].

2.2. Techniques

Differential thermogravimetric analysis (DTA) was performed on a Stanton Redcroft 673-4 thermoanalyser in static air atmosphere. Thermoheated samples at several temperatures were obtained by interrupting the DTA experiment; these samples were used in the remaining determinations. X-ray diffraction patterns were obtained at room temperature with a Siemens D501 diffractometer with a CuK_α radiation and a graphite monochromator. The fraction of anatase, X_A, was calculated from the following expression [11]

$$X_A = \frac{1}{1 + 2.18\,(I_R/I_A)} \pm 2\% \qquad (1)$$

* Author to whom all correspondence should be addressed.

0022–2461

where I_R and I_A are the intensities of the reflections for the (1 1 0) plane of rutile and the (1 0 1) plane of anatase, respectively, as measured from the total area of the peaks. These diffraction lines were suited for measurement of the intensity ratio because of their strong intensity and their symmetrical shape.

Scanning electron microscopy (SEM) was carried out in an ISI apparatus, model SS40, and the dispersion energy of X-rays was measured by a Kevex analyser model 8000; a semiautomatic image analyser of magnetostrictive board Kontron MOP-30 was used to estimate the weight average size of aggregates and particles.

Characterization of the surfaces was carried out using a combination of temperature-programmed desorption (TPD), infrared spectroscopy and thermogravimetric analysis (TG). The infrared spectra were recorded on a Perkin–Elmer model 883, the specimens being embedded in a KBr disc. The non-isothermal thermogravimetric traces were recorded under a vacuum $< 10^{-3}$ torr (1 torr = 1.333×10^2 Pa) using a Cahn Electrobalance, model RG, and heating rate of 4 K min^{-1}. The evolved gas analysis (EGA) during heating of the sample was performed (under vacuum, $< 10^{-3}$ torr) by attaching the sample tube to a mass spectrometer (MS) equipped with a quadrupole sensing head model QF-200 with a Faraday-cup detector; a heating rate of 4 K min^{-1} was used.

3. Results

3.1. TPD–MS/TG and DTA study

Fig. 1a shows the TPD profiles of water desorbing from iron-doped specimens. All samples showed desorption peaks below 573 K with relatively slight differences except for the relative intensities of the same peaks which have different intensity values from one sample to another; these peaks should reflect the different types of adsorbed molecular water. In order to quantify the total amount of desorbed molecular water below 673 K, TG technique has been applied. Thermogravimetric traces from the above specimens are plotted in Fig. 1b. According to TG diagrams, the percentage weight loss up to 673 K, which may be related to the water peaks from TPD, are very similar for all samples with only minor differences between them (0.64%–0.72%). It is worthy of note that the percentage weight loss slightly increases in the following sequence: (IM) 0.5/773 < (IM) 5/773 < (IM) 1/773 < (IM) 2/773. The above sequence could be explained in terms of differences in "external" surface areas measured and previously reported [3]. It should be noted, however, that TPD–MS analysis for the (IM) 0.5/773 sample showed a characteristic desorption peak with a maximum at 523 K corresponding to $\sim 1\ H_2O\ nm^{-2}$ which is absent or more discrete in the other more concentrated iron samples; it is remarkable that this water peak, which is desorbing in the temperature range 498–573 K is larger in the (IM) 0.5/773 sample even if the total molecular water desorbed from this sample is smaller, compared to the other more concentrated iron samples.

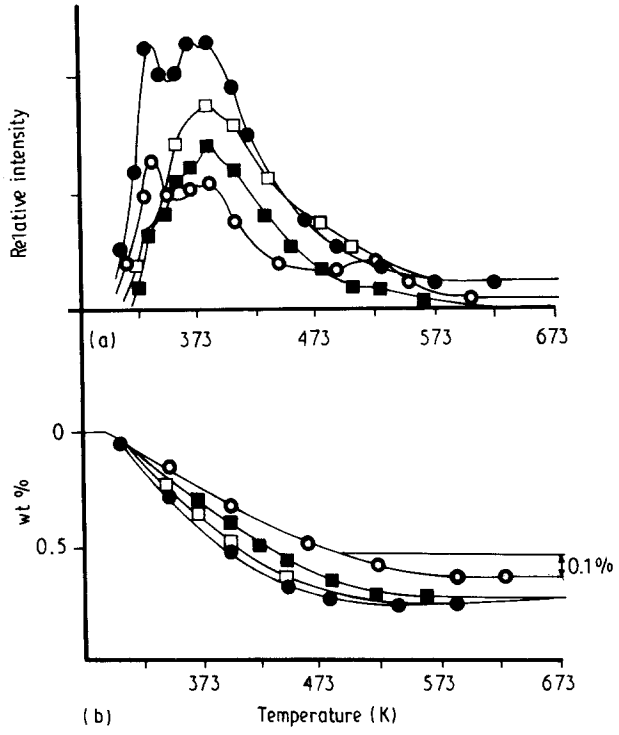

Figure 1 (a) TPD profiles and (b) TG curves (water evolution) of the studied iron-doped titania specimens. All samples were previously calcined at 773 K, 24 h; $\beta = 4$ K min^{-1}, 10^{-3} torr. (○) (IM) 0.5/773, (□) (IM) 1/773, (●) (IM) 2/773, (■) (IM) 5/773.

The thermal evolution by DTA for the starting undoped and iron-doped titania powders, is shown in Fig. 2. The first endothermic effect at 380 K is ascribed to the elimination of adsorbed molecular water from the surface of the powdered materials, as indicated by the TPD–MS results. As thermal treatment increases, the remaining water, strongly bonded inside the pores of the particles, can then be eliminated thus giving the second overlapping endothermic effect at 450 K. In fact, according to previous results [3] the loss of adsorbed molecular water in the range 373–573 K appears to be related to the development of porosity.

For iron-doped titania samples, a third endothermic peak at $\sim$ 660 K was observed. This peak is due to the thermal decomposition of the adsorbed precursor nitrate species, as analysed using infrared spectroscopy and TPD–MS experiments [12]. In addition, an exothermal effect at 1043 K was observed; this exothermic effect, which was not observed on pure TiO_2, may be related with the presence of iron on the TiO_2 matrix.

Finally, the loss of water from the condensation of surface hydroxyl groups [13] at temperatures higher than 573 K must account for the commencement of the sintering process observed by DTA from 623 K.

3.2. Bulk information by XRD technique

Table I summarizes the variation in the weight fraction of anatase, X_A, for the starting undoped and precursor iron-doped titania specimens, just before and after the sharp exothermic DTA peak (Fig. 2). For iron-doped TiO_2 specimens it may be observed (Table I) that at 973 K the X_A fraction slightly increases with increasing iron content. In the case of

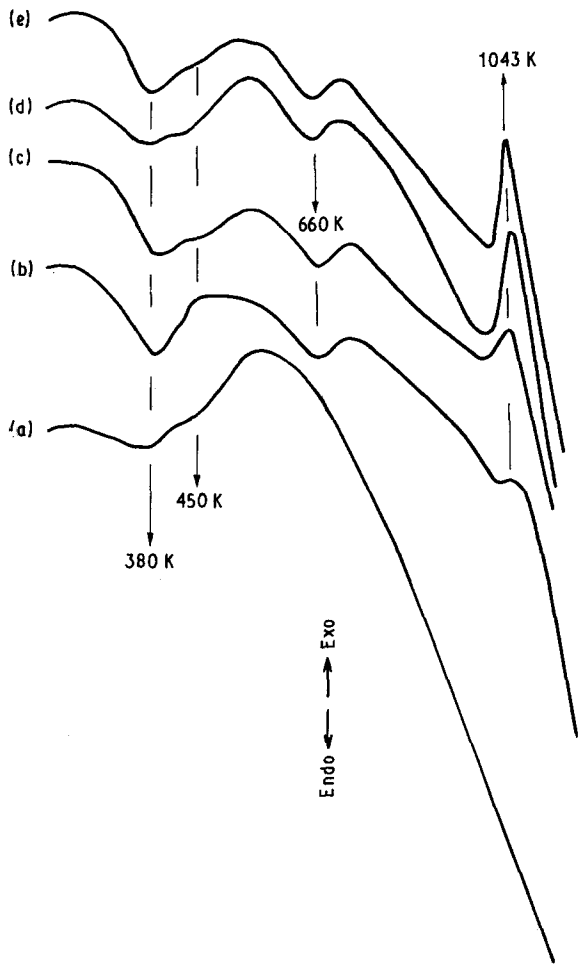

Figure 2 DTA curves of the as-prepared undoped and iron-doped titania specimens: (a) pure TiO_2; (b) Fe/TiO_2 (0.5% Fe^{3+}); (c) Fe/TiO_2 (1% Fe^{3+}); (d) Fe/TiO_2 (2% Fe^{3+}); (e) Fe/TiO_2 (5% Fe^{3+}); $\beta = 10\ K\ min^{-1}$.

TABLE I Weight fraction of anatase, X_A in the studied compounds just before and after the exothermic peak (DTA) at 1043 K

Starting materials	973 K	1073 K
Undoped TiO_2	0.488	0.145
Fe/TiO_2 (0.5% Fe^{3+})	0.481	0.064
Fe/TiO_2 (1% Fe^{3+})	0.516	0.022
Fe/TiO_2 (2% Fe^{3+})	0.518	0.022
Fe/TiO_2 (5% Fe^{3+})	0.543	0.022

Note: the weight fraction of anatase in the original TiO_2 sample was $X_A \approx 0.602$.

undoped TiO_2, a relatively important amount of anatase ($X_A = 0.145$) remains present after cut off from the DTA at 1073 K. However, on iron-doped TiO_2, just after the exothermic peak, rutile was clearly identified from the sharp X-ray peaks as the main crystalline phase, in addition to the presence of a very small amount of anatase, which is practically negligible ($X_A = 0.022$–0.064). Thus, the exothermic DTA peak observed for iron-doped titania samples is associated with a drastic polymorphic transformation, anatase–rutile, at 1043 K, which seems to be accelerated by the presence of Fe^{3+} ions, as reported in the literature [14].

The structural features of pure TiO_2 and iron-doped TiO_2 specimens calcined at different temperatures for 24 h have also been investigated by XRD technique and the results are summarized in Table II. At temperatures below 1073 K, pure TiO_2 always exhibits anatase phase, although the relative amount of anatase compared to rutile decreases with increasing calcination temperature. However, for iron-doped titania specimens, only a lesser amount of anatase phase remains present, compared with undoped TiO_2, after prolonged calcination at 923 K, the transformation of anatase into rutile being completed after prolonged firing at 1073 K. In addition, for specimens with iron contents higher than 2%, thermal treatment at $T > 1073$ K causes the appearance, on the X-ray powder pattern, of reflections of a disordered phase, identified as pseudobrookite, Fe_2TiO_5 (see Fig. 3b), which is not observed for more diluted iron samples (see Fig. 3a).

On the other hand, we note from Table II that at each of the calcination temperatures, the X_A fraction of the starting TiO_2 matrix is significantly altered by the presence of iron, but this alteration seems to be independent of the nominal concentration of iron. It is also noteworthy that the differences observed for the X_A fraction between Table I (at 973–1073 K) and Table II (at 923–1073 K) clearly indicate that the transformation of anatase into rutile phase is accelerated not only by the presence of iron but also by a time-dependent kinetic effect.

TABLE II Summarized results of the weight fraction of anatase X_A, in the studied compounds calcined for 24 h at the indicated temperatures

Samples	773 K	923 K	1073 K	1273 K
Undoped TiO_2	0.518	0.084	0.022	0.000
Fe/TiO_2 (0.5% Fe^{3+})	0.442	0.048	0.000	0.000
Fe/TiO_2 (1% Fe^{3+})	0.442	0.052	0.000	0.000
Fe/TiO_2 (2% Fe^{3+})	0.444	0.043	0.000	0.000
Fe/TiO_2 (5% Fe^{3+})	0.452	0.052	0.000	0.000

Note: the weight fraction of anatase in the original TiO_2 sample was $X_A \approx 0.602$.

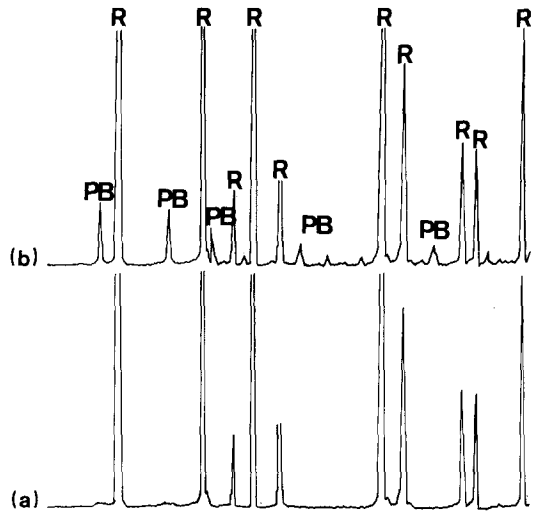

Figure 3 X-ray diffraction diagrams of iron-doped titania samples: (a) (IM) 0.5/1273, (b) (IM) 5/1273.

3.3. Surface information from infrared spectroscopy

The infrared spectra of iron-doped TiO_2 samples calcined at 773 K (24 h) show a broad band in the region from 3600–2600 cm^{-1} (O–H stretching mode vibration) with a maximum at about 3300 cm^{-1} (see Fig. 4a), accompanied by a small band at 1620 cm^{-1} (H–O–H bending mode vibration), (see Fig. 4b) indicating that this sample contains loosely adsorbed water molecules, heterogeneously distributed, in agreement with TPD results; no peak at 3730 cm^{-1}, characteristic of basic hydroxyl groups, OH^- [15], was observed.

Fig. 4c shows the 1200–400 cm^{-1} absorption region in the infrared spectra for iron-doped titania specimens calcined at 773 K. All spectra showed peaks at 810, 605, 585, 525 and 430–410 cm^{-1}. Moreover, a shoulder at about 460 cm^{-1} appeared in those samples containing a nominal concentration of iron, > 1%; furthermore, the (IM) 5/773 specimen shows two small peaks at about 850 and 950 cm^{-1} plus one other at 1165 cm^{-1}. Artificial anatase and rutile have large broad bands in the 850–530 cm^{-1} region which mask their characteristic bands at 810 and 603 cm^{-1} [16]; additional bands at 425–430 cm^{-1} and 525–530 cm^{-1} are also present on artificial anatase and rutile. Bands at 1165, 950. 850 and 585 cm^{-1} could be tentatively ascribed to brookite phase, because they have been found in brookite [16] which is distinguished from other phases by its band at 1165 cm^{-1}. The assignment of the band at 460 cm^{-1} requires greater attention; even bands at 450–460 cm^{-1} can be present in anatase, rutile and brookite phases [16]; however, its absence in the (IM) 0.5/773 sample suggests that it could be related to the presence of iron in concentrations greater than 1%. In fact, bands at 450–460 cm^{-1} are characteristic of iron minerals, e.g. α-Fe_2O_3 [16].

3.4. SEM–EDX study

SEM technique showed that iron-doped titania samples calcined at 773 K consist of very fine free individual grains plus other granular aggregates (see Fig. 5a as a representative of the SEM results); very large distributions of shape and dimensions of the particles were observed. EDX analysis of iron-doped samples calcined at 773 K showed that the granular aggregates contain iron, not uniformly distributed between particles, nor within one particle, whereas the small (~ 5 μm) free individual grains (Fig. 5b) are pure TiO_2. Although the large (~ 100 μm) aggregates (Fig. 5a) have straight edges and sharp corners, it is, however, correct to call them aggregates because a detailed examination by SEM (Fig. 6a) showed that they are really formed by particles of very irregular shape and dimensions. However, a detailed SEM examination of the smaller free individual grains (Fig. 6b) showed that

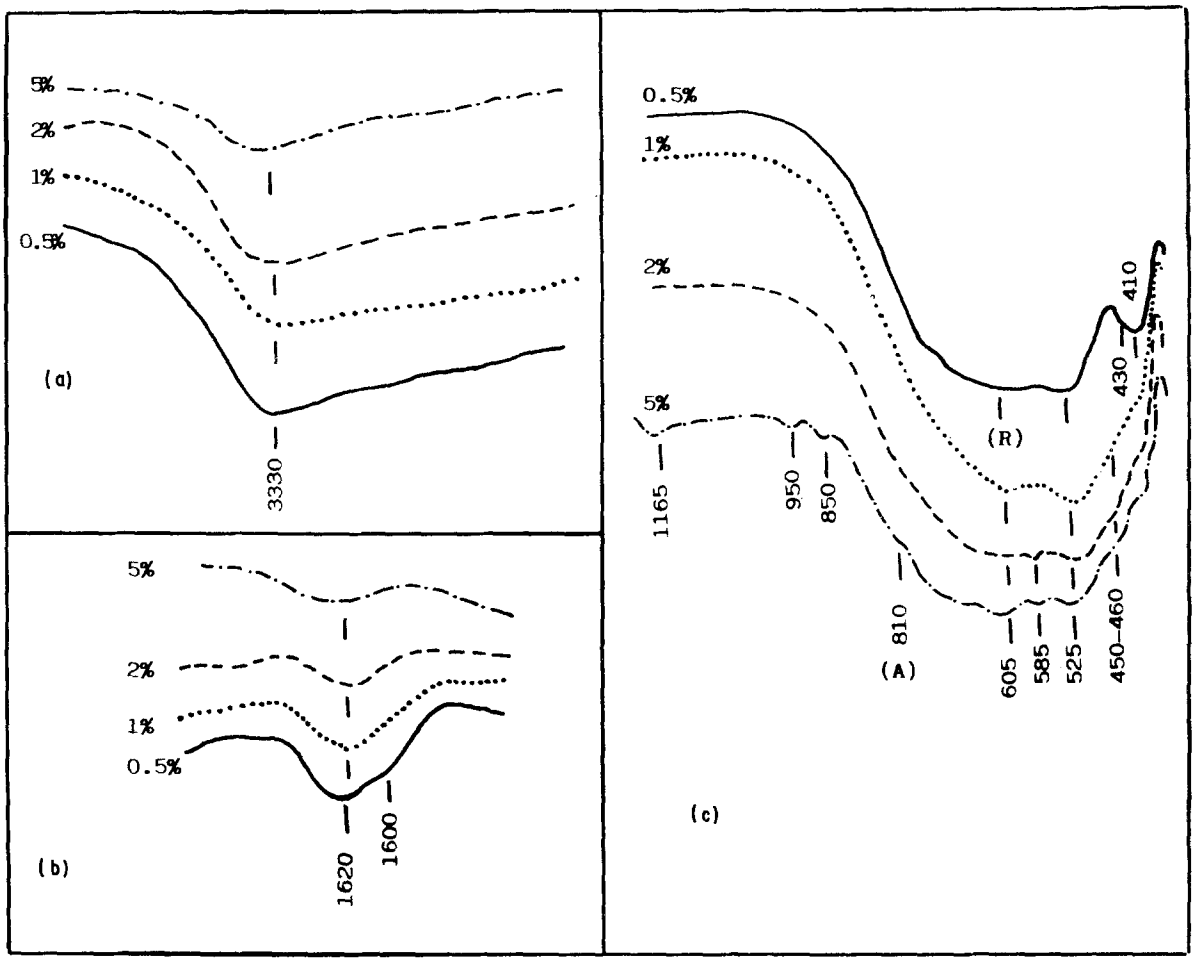

Figure 4 Infrared spectra of iron-doped titania samples containing the indicated percentage of Fe^{3+} ions. All samples were previously calcined at 773 K, 24 h.

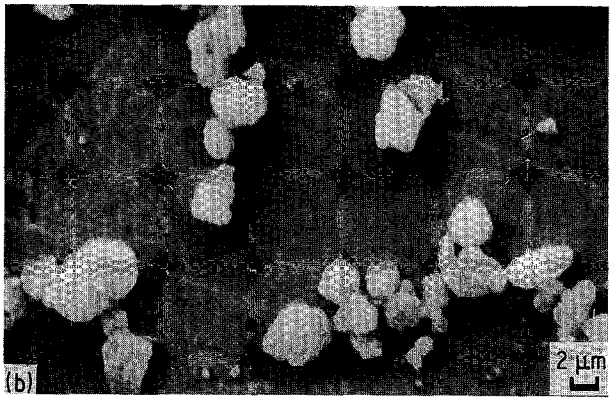

Figure 5 (a) Scanning electron micrograph of an (IM) 5/773 sample showing aggregates and free individual particles; (b) detail of the smaller particles shown in (a).

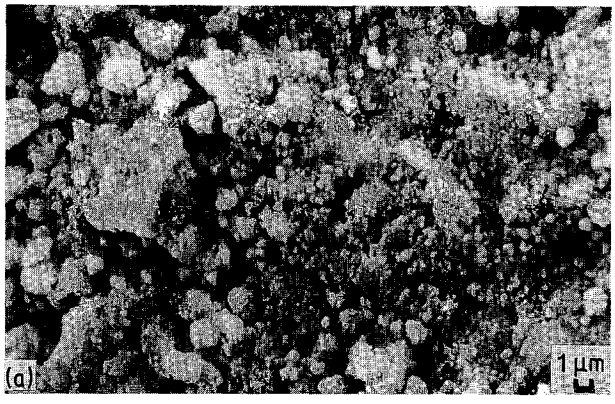

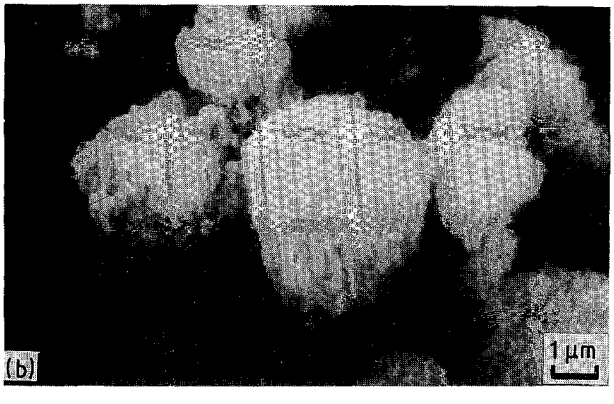

Figure 6 Fig. 5a and b at higher magnification.

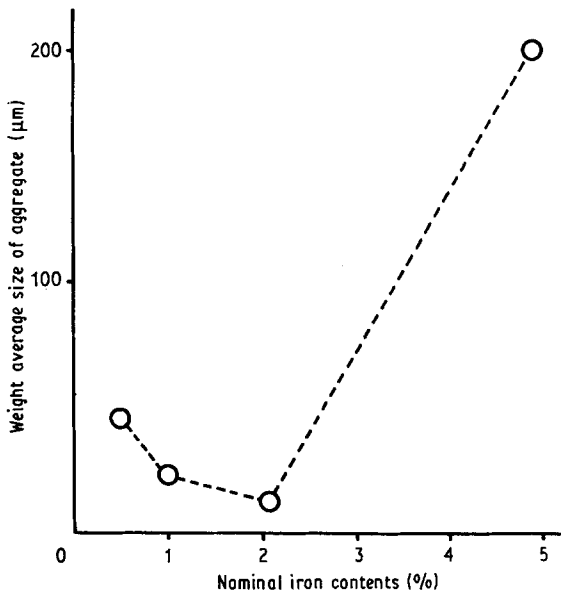

Figure 7 Weight average size of aggregates for iron-doped titania samples (previously calcined at 773 K, 24 h) as a function of the nominal iron content.

they are homogeneous, regular, and approximately spherical shaped particles of pure TiO_2.

Fig. 7 shows the weight average size of aggregates for the iron-doped TiO_2 specimens calcined at 773 K compared with the nominal iron contents; a slight decrease in the weight average size of aggregates is observed up to 2% of Fe^{3+}, which then increased for larger iron concentrations (e.g. 5% Fe^{3+}).

When iron-doped TiO_2 samples were heat treated for prolonged times at 923, 1073 and 1273 K, SEM examination showed (Fig. 8) the progressive development of crystallinity. According to DTA–XRD results, for iron-doped titania samples, exothermic peaks were observed which correspond to a drastic transformation of anatase into rutile phase. At 1073 K sintering was observed (see Fig. 2) to cause crystallites (see Fig. 8b) to coalesce and to grow in size (Fig. 8c); this, of course, has the undesirable effect of reducing the surface area of these samples, as reported in a previous paper [3].

4. Discussion

Without any thermal pretreatment, the commercial TiO_2 (Degussa, P-25) has been shown to be 80% anatase and 20% rutile; however, the anatase/rutile ratio (A/R) is strongly dependent on the history of the sample, the anatase fraction, X_A of our starting TiO_2 sample being found to be about 0.602.

After calcination treatments, the initial A/R ratio on TiO_2 decreases because the transformation of anatase into rutile is decreasingly effective after prolonged calcination treatments, even at 773 K. During the calcination processes of the different as-prepared iron-doped TiO_2 materials, the pre-adsorbed precursor nitrate is decomposed and the iron ions, initially present at the surface, diffuse into the bulk and could produce solid solution, the extent of this process being controlled by the A/R ratio in the TiO_2 matrix for all

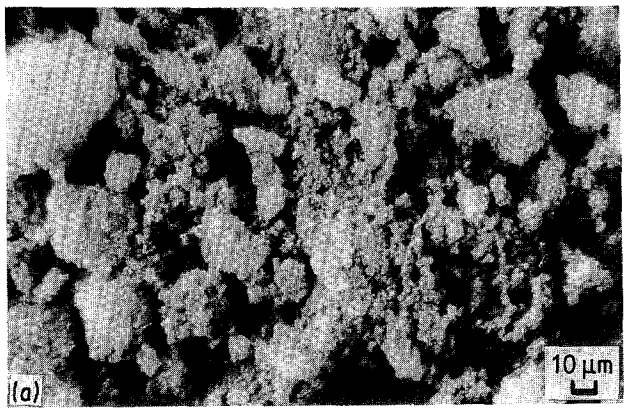

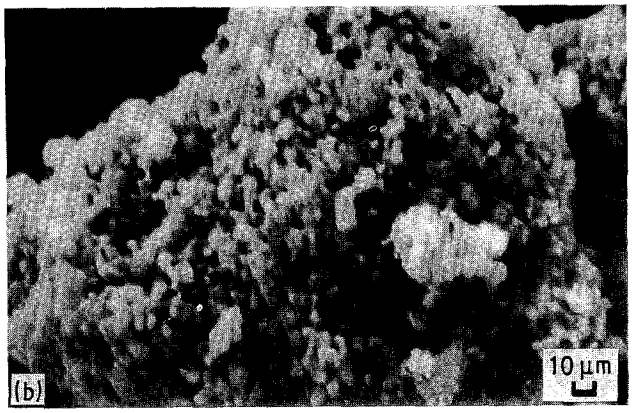

Figure 8 Scanning electron micrographs of the iron-doped titania sample (5% Fe^{3+}) after calcination for 24 h at (a) 923 K, (b) 1073 K, (c) 1273 K.

calcination temperatures and by the solubility of iron in both phases.

The solubility of Fe^{3+} ions in anatase phase is greater than in rutile. Although previous results using ESR have indicated [17] that the solubility limit of Fe^{3+} in rutile is $< 0.5\%$, recent results [18] have shown, however, that Fe^{3+} ions are incorporated into the rutile phase in a limited amount of 1.2–1.4 Fe atoms/100 Ti atoms, thus corresponding to $\sim 0.92\%$ Fe. The discrepancy between both sets of results has been ascribed [18] to the fact that, according to the literature [19, 20] only a fraction of Fe^{3+} in the solid solution is detectable by ESR.

Previous photocatalytic results have shown [5–7] that catalysts with an iron content of 0.2%–0.5% calcined at 773 K are the most active samples.

After a prolonged thermal treatment at 773 K, the iron-doped titania samples contain a relatively important amount of anatase phase, the fraction X_A being more or less independent of the nominal concentration of iron (see Table II). Thus, the observed differences in the photocatalytic activity between iron samples calcined at 773 K should be linked not only to the anatase/rutile ratio but also to the nominal iron content. In fact, infrared results have shown (Fig. 4c) that for specimens with iron concentrations greater than 1%, iron oxide is observed at the surface. These results could indicate that after prolonged calcination treatments at 773 K, only samples containing iron concentrations lower than 1% can produce solid solutions; iron that cannot be accommodated in solid solution is segregated to form a surface layer of iron oxide, and/or reacts, by thermal treatment, with TiO_2 forming Fe_2TiO_5 as a separated phase. XRD and infrared spectroscopy data support this interpretation. By increasing the calcination temperature, the drastic transformation of anatase into rutile phase, which is accelerated by the presence of iron [14] may produce a segregation of iron and, subsequently, a thermal reaction with TiO_2, forming Fe_2TiO_5 as a separated phase; for $T > 773$ K this effect could be more pronounced on samples with iron contents greater than 1%, because this is the limiting amount from which iron oxide is observed (infrared results) on the specimens, even after prolonged calcination at 773 K. In fact, traces of Fe_2TiO_5 have been observed, even on sample (IM) 2/923, and a relatively important amount of the pseudobrookite phase has been detected by XRD on the (IM) 5/1273 sample (see Fig. 3).

It should be noted that SEM and EDX studies have shown that this photocatalyst consists of aggregated particles with a non-uniform distribution of iron and other free pure TiO_2 particles; this behaviour reflects that, even below the limit of solubility of iron in anatase, it is possible that, as the impregnation method is not properly suited for a uniform distribution of iron, particles with iron above the solubility limit could be formed, even for initial concentrations of iron $< 1\%$. In any case, the excess iron which is segregated to the surface could, probably, facilitate the interaction between particles, thus giving aggregates. In fact, as shown in Fig. 7, the weight average size of aggregates is greater for samples containing larger concentrations of iron ($> 2\%$).

The presence of pseudobrookite phase and/or iron oxide in our Fe/TiO_2 specimens containing a high proportion of iron ($> 1\%$) and/or fired at elevated temperatures, must account for the differences observed in each sample's ability to photo-reduce dinitrogen to ammonia. In fact, we have proved [21] that the reduction of MV^{2+} (methyl viologen) by conduction band electrons is more feasible on the (IM) 0.5/773 sample, in which pseudobrookite is not present, than in (IM) 5/773 or pure TiO_2 samples. The same points have been given in a recent paper by Navio *et al.* [10] to explain differences between undoped and iron-doped titania catalysts on the photocatalytic oxidation of neat liquid toluene.

Acknowledgements

This work was supported by "Junta de Andalucia" (financial support for research groups/1990). We also thank Mr E. Gomez for the SEM–EDX facilities.

References

1. M. SCHIAVELLO and A. SCLAFANI, in "Photoelectrochemistry, Photocatalysis and Photoreactors", edited by M. Schiavello, NATO-ASI, Series C, Vol. 146 (D. Reidel, Dordrecht, Holland, 1985) p. 503.
2. R. I. BICKLEY and J. A. NAVIO, in "Photocatalytic Production of Energy-Rich Compounds", edited by G. Grassi and D. O. Hall (Elsevier, London, 1985) p. 105.
3. R. I. BICKLEY, T. GONZALEZ-CARREÑO and L. PALMISANO, in "Preparation of Catalysts IV", Vol. 31, edited by B. Delmon, P. Grange, P. A. Jacobs and G. Poncelet (Elsevier, Amsterdam, 1987) p. 297.
4. G. N. SCHRAUZER and T. D. GUTH, *J. Amer. Chem. Soc.* **99** (1977) 7189.
5. V. AUGUGLIARO, A. LAURICELLA, L. RIZZUTI, M. SCHIAVELLO and A. SCLAFANI, *Int. J. Hydrogen Energy* **7** (1982) 845.
6. V. AUGUGLIARO, F. D'ALBA, L. RIZZUTI, M. SCHIAVELLO and A. SCLAFANI, *ibid.* **7** (1982) 851.
7. M. SCHIAVELLO, L. RIZZUTI, R. I. BICKLEY, J. A. NAVIO and P. L. YUE, in "Proceedings of the International Congress on Catalysis", Vol. III (Verlag Chemie, Basel, Berlin, 1980) p. 383.
8. G. N. SCHRAUZER, T. D. GUTH, J. SALEHI, N. STRAMPACH, LIU NAN HUI and M. R. PALMER, in "Homogeneous and Heterogeneous Photocatalysis", edited by E. Pelizzetti and N. Serpone (Reidel, Dordrecht, Holland, 1986) p. 509.
9. J. C. CONESA, J. SORIA, V. AUGUGLIARO and L. PALMISANO, in "Structure and Reactivity of Surfaces", edited by C. Morterra, A. Zecchina and G. Costa (Elsevier, Amsterdam, 1989) p. 30.
10. J. A. NAVIO, M. GARCIA GOMEZ, M. A. PRADERA and J. FUENTES MOTA, in Proceedings of the 2nd International Symposium on Heterogeneous Catalysis and Fine Chemicals II, published in Studies in Surface Science and Catalysis **59** (Elsevier, Amsterdam, 1991) p. 445.
11. M. CRIADO, C. REAL and J. SORIA, *Solid State Ionics* **32/33** (1989) 461.
12. J. A. NAVIO, A. JUSTO, M. MACIAS and C. REAL, unpublished results (1991).
13. G. MUNUERA and F. S. STONE, *Disc. Farad. Soc.* **52** (1971) 205.
14. Y. IIDA and S. OZAKI, *J. Amer. Ceram. Soc.* **44** (1961) 120.
15. G. MUNUERA, V. RIVES-ARNAU and A. SAUCEDO, *JCS Farad. Trans. I* **75** (1979) 736.
16. H. W. VAN DER MAREL and H. BEUTELSPACHER, in "Atlas of Infrared Spectroscopy of Minerals and their Admixtures" (Elsevier, Amsterdam, 1976) p. 257.
17. D. GORDISCHI, N. BURRIESCHI, F. D'ALBA, M. PETRERA, G. POLIZZOTTI and M. SCHIAVELLO, *J. Solid State Chem.* **56** (1985) 182.
18. D. GAZZOLI, G. MINELLI and M. VALIGI, *Mater. Chem. Phys.* **21** (1989) 93.
19. P. O. ANDERSON, E. L. KOLLBERG and A. JELENSKI, *J. Phys.* **C7** (1974) 1868.
20. J. S. THORP, H. S. EGGLESTON, T. A. EGERTON and A. J. PEARMAN, *J. Mater. Sci. Lett.* **5** (1986) 54.
21. J. A. NAVIO, F. J. MARCHENA, M. RONCEL and M. A. de la ROSA, *J. Photochem. Photobiol. A, Chem.* **55** (1991) 319.

Received 6 February
and accepted 14 June 1991